Fusion of Gabor Filter and Co-occurrence Probability Features for Texture Recognition

David A. Clausi, Huawu Deng
Systems Design Engineering, University of Waterloo
dclausi@engmail.uwaterloo.ca, h2deng@rousseau.uwaterloo.ca

Abstract

This paper explores a design-based method to fuse Gabor filter features and co-occurrence probability features for improved texture recognition. The fused feature set utilizes both the Gabor filter's capability of accurately capturing lower frequency texture information and the co-occurrence probability's capability in texture information relevant to higher frequency components. Fisher linear discriminant analysis indicates that the fused features have much higher feature space separation than the pure features. Image texture segmentation results are presented that also demonstrate the improvement using the fused feature sets.

1 Introduction

Image segmentation is the task of labelling regions in an image. There is no known method that is able to consistently and accurately segment texture images. A commonly used strategy for texture segmentation is first to extract texture features on a pixel-by-pixel basis from a texture image and then perform a clustering technique on the extracted texture features [1].

Many scientists have considered the problem of extracting texture features. Tuceryan and Jain [1] classified texture feature extraction methods into four categories: statistical, geometrical, model-based, and signal processing methods. Co-occurrence probability features (a statistical-based method) have been demonstrated to be preferred in a classification sense when compared with Fourier power spectrum features, second order gray level statistics and gray level run length features [2][3]. Gabor filters (a signal processing method) have also demonstrated their efficiency in characterizing texture information for segmentation purposes [4]. These different kinds of texture features alone might, however, have limited power for describing textures. Fusion of different texture features is therefore suggested to improving performance of information representation.

Solberg and Jain [5] fused co-occurrence probability features, local statistics features, fractal features and random field features for image classification. Clausi [6] combined the features from co-occurrence probabilities, Gabor filters and Markov random fields for classification purpose. Fusion allows use of all available features or an optimal subset of all features according to the feature data set itself. This paper explores a design-based method for feature fusion. The idea is that the theoretical properties of each feature is examined in order to select the robust and reliable features for fusion. The Fisher linear discriminant method will be used to estimate the separability of classes in the feature space using one of the prescribed feature sets. The fusion of co-occurrence probability features and Gabor filter features is considered in this paper.

Gabor filters respond strongly to frequencies that match the Gabor filter frequency. However, in the presence of impulsive noise, high frequency Gabor filters generate highly variable features. Co-occurrence probability features, on the other hand, are not as sensitive to impulsive noise and are not appropriate for estimating lower frequency features. The fusion of low and medium frequency Gabor filter features and high frequency co-occurrence features is expected to generate an improved feature set.

The rest of the paper is organized as follows. Sections 2 and 3 introduce Gabor filters and co-occurrence probabilities. Section 4 discusses a basis for fusing the texture features. Section 5 shows the results of cluster separability and segmentation experiments. Section 6 concludes the paper.

2 Gabor Filters

Research has demonstrated that the human visual system (HVS) is sensitive to both specific orientations and spatial frequencies [7] [8]. For texture anal-

ysis, wavelets have the ability to model the frequency and orientation sensitivity characteristic of the HVS [9]. A Gabor filter bank can be designed to mimic a wavelet filter bank. Due to its appealing simplicity and optimum joint spatial/spatial-frequency localization, the Gabor function is attractive for computer vision applications, especially texture segmentation [4] [10].

A Gabor function is a Gaussian modulated complex sinusoid in the spatial domain [4]. The 2-D Gaussian has an aspect ratio of σ_x/σ_y. The complex exponential has a spatial frequency of F and an orientation θ (counterclockwise with respect to the horizontal axis). Rotation in the plane then provides for any arbitrary orientation of the filter. The mathematical tractability of the Gabor filter in the spatial-frequency domain is appealing since it is simply a Gaussian centered on the frequency of interest eg.

$$H(u,v) = \exp\left[-2\pi^2\left((u-F)^2\sigma_x^2 + v^2\sigma_y^2\right)\right]. \quad (1)$$

There are six parameters that must be set when implementing a Gabor filter bank: $F, \theta, \sigma_x, \sigma_y, B_F$ and B_θ. B_F are B_θ are the frequency and angular bandwidth respectively. Details on how to set these parameters are determined is found in [4][10][11]. Although there exist many techniques to extract features from Gabor filter outputs, the magnitude response is a preferred method [11] and will be used exclusively here. Bovik *et al* [10] pointed out that textures which do not have sufficiently narrow bandwidths suffer from "leakage". The effects of leakage can be reduced by post-filtering the channel amplitudes with Gaussian filters having the same shape as the corresponding channel filters but greater spatial extends. It is therefore necessary to apply Gaussian smoothing over the magnitude responses to improve the performance of Gabor filters. Smoothing has been performed in this paper using the method advocated by Bovik et al.

3 Co-occurrence Probabilities

The co-occurrence matrix proposed by Haralick *et al* [12] is a common method for texture feature extraction. It consists of co-occurring probabilities of all pairwise combinations of grey levels (i,j) in the fixed-size spatial window given two parameters: inter-pixel distance (δ) and orientation (θ). These two terms together with gray level quantization and window size determine the co-occurrence probabilities, which are stored in the co-occurrence matrix. Statistics are applied to the co-occurrence probabilities to generate texture features. Generally, these statistics identify some structural aspect of the arrangement of co-occurring probabilities stored within a matrix indexed on i and j, which in turn reflects some qualitative characteristic of the local image texture (eg. smoothness or roughness). There are many statistics that can be used, however, only three statistics are advocated for shift-invariant applications since these should generate preferred discrimination with the least redundancy [13]. The selected statistics are contrast (CON), entropy (ENT), and correlation (COR).

Coarser quantization can accelerate calculation of the co-occurrence features and reduce noise but, at the same time, lose texture information. The work in [14] and [15] supports a quantization level of 64. The window size determines the ability to capture texture features using different spatial extends. If the window size is smaller than the size of a texture primitive, the co-occurrence method might not capture the characteristics of the texture primitive. For a segmentation problem, however, the larger the window size, the greater the risk that multiple textures will appear in the window and produce misleading features. The window size in this paper will be chosen to match the Gabor filter spatial extent.

4 Feature Fusion

4.1 Theoretical Analysis

A common strategy of feature fusion is first to combine various features and then perform feature selection to choose an optimal feature subset according to the feature data set itself, such as by principal component analysis (PCA). This paper considers a design-based method for feature fusion. Here, strengths and weaknesses of each method are examined in theory. Then, texture features are selectively fused according to their compatibility.

Gabor filters, implemented in a pseudo-wavelet scheme, are able to describe texture information in low and medium frequencies but have problems in describing high frequency information in the presence of impulsive noise. The higher the frequency of a Gabor filter, the more sensitive the filter is to the impulsive noise. This is due to the higher frequency filters having larger spatial-frequency bandwidth which covers more impulsive noise that is evenly distributed in the spatial-frequency domain.

An example of the impact of additive white noise on the feature extraction ability of Gabor filters is

presented. Long duration sinusoids of frequencies ranging from 2 to 24 pixels per cycle (ppc) were created and zero mean noise ($\sigma = 0.2$) was added to each signal. A Gabor filter with a matched frequency was convolved with each signal and the magnitude response determined. The standard deviation of the magnitude response was determined in each case and plotted in Fig. 1. With higher local frequencies (smaller ppc), the standard deviation increases tremendously indicating that the Gabor filter estimates at high frequency are not accurate.

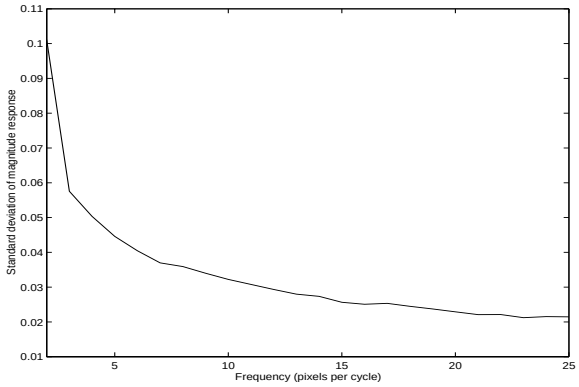

Figure 1: *The change of standard deviation of the magnitude response with respect to the matched signal and filter frequency.*

To replace the high-frequency Gabor filter features with some other more suitable features is appropriate. The co-occurrence probability features are able to play such a role. If the inter-pixel distance is set to 1 or 2 at different orientations, the corresponding co-occurrence probability features measure local high frequency information. The co-occurrence probability method assumes a uniform distribution across the window of interest as opposed to Gabor filters which weight the local region using a Gaussian function. As a result, the co-occurrence method is not as susceptible to local additive noise. Fusing the medium and low frequency Gabor filter features and the high frequency co-occurrence features is expected to generate an improved feature set.

4.2 Feature Normalization For K-Means Clustering

The K-means clustering method [16] is employed here to cluster feature vectors to generate a segmented image. As the K-means clustering method is generally implemented according to the criterion of minimizing the Euclidian distance between feature vectors, it is necessary to normalize the fused features. The normalization should comply with a rule that each feature component should be treated equally for its contribution to the distance. The rationale usually given for this rule is that it prevents certain features from dominating distance calculations merely because they have large numerical values. As the feature vectors for segmentation are spread due to the presence of subclasses, it can be quite inappropriate to normalize the feature vector to be of zero mean and unit variance [16]. This paper uses a linear stretch method to normalize each feature component over the entire data set to be between zero and one.

A feature selection procedure can be used after the feature vectors are fused. In this paper, a weighting method called feature contrast [17] is employed to perform an unsupervised feature selection. Pichler *et al* [17] defined the feature contrast as an indicator of the difference between different texture regions. They developed this concept originally for Gabor filter feature selection and weighting. This paper applies the method not only to the selected Gabor filter features but also to the co-occurrence probability features.

Denote the i-th n-D fused feature vector as $F_i = \{f_{i,1}, f_{i,2}, \cdots, f_{i,n}\}$. The feature contrast of the j-th component of the feature vector is defined as:

$$\xi_j = \frac{\max_i(f_{i,j}) - mean_i(f_{i,j})}{\max_i(f_{i,j}) + mean_i(f_{i,j})}. \qquad (2)$$

Then each feature component is weighted by its feature contrast divided by the maximum feature contrast of all feature components, that is, $F_i^* = \frac{1}{\max_j(\xi_j)}\{\xi_1 f_{i,1}, \xi_2 f_{i,2}, \cdots, \xi_n f_{i,n}\}$.

5 Experimental Results

5.1 Testing Methodology

The test image (256×256 pixels), shown in Fig. 2(a), contains Brodatz textures [18] and was previously published in [19]. Its seven textures, introduced in raster order, are canvas (D021), field stone (D002), shaw cloth (D052), wood grain (D068), fiber cloth (D076), netting (D034) and wire (D006).

A total of 24 complex Gabor filters at four frequencies (22.63 ppc, 11.31 ppc, 5.66 ppc, 2.83 ppc) (corresponding to the frequencies $8\sqrt{2}$, $16\sqrt{2}$, $32\sqrt{2}$, $64\sqrt{2}$ cycles per image for a 256×256 image) and six orientations (0^o, 30^o, 60^o, 90^o, 120^o, 150^o) are chosen to filter the test image. The magnitude of

Table 1: *Denotations of texture feature sets.*

F_{G18}	The feature set using the 18 Gabor filter features at the three lowest frequencies.
F_{G24}	The feature set using all 24 Gabor filter features.
F_{C24}	The feature set using all 24 co-occurrence probability features.
F_{G18}^{C24}	The feature set fusing F_{G18} and F_{C24}.
F_{G24}^{C24}	The feature set fusing F_{G24} and F_{C24}.

each filtered image will be smoothed by an amplitude Gaussian (the scale is 2/3 [10]). Thus a 24-D Gabor filter feature vector can be obtained for each pixel. The feature set using the 18 Gabor filter features at the lowest frequencies is denoted by F_{G18}, and the feature set using all 24 Gabor filter features is denoted by F_{G24} in this paper.

As the 2.83 ppc Gabor filter is sensitive to impulsive noise in an image, the related Gabor filter feature will be discarded in feature fusion. As a result, a 9×9 window can cover most energy of the 2.83 ppc Gabor filter given $\pm 3\sigma$ ($\sigma = 1.59$ pixels), so this window size is used exclusively. By choosing two inter-pixel distances ($\delta = 1, \delta = 2$) and four orientations (0^o, 45^o, 90^o, 135^o), a total of eight co-occurrence matrices can be calculated for each pixel. The three statistics (ENT, CON, COR) are applied to each set of co-occurring probabilities. Thus, each pixel is represented by a 24-D co-occurrence probability feature vector. The feature set using these 24 co-occurrence probability features is denoted by F_{C24}.

The fusion is performed by combining the F_{G18} with the F_{C24}. This fused feature set is denoted by F_{G18}^{C24}. Another fusion is to combine the F_{G24} with the F_{C24} for comparison. This fused feature set is denoted by F_{G24}^{C24}. The denotations of all five feature sets are listed in Table 1.

The first step of the test is the discriminant analysis. Fisher linear discriminant (FLD) is employed as it is a recognized method to analyze the separation ability between classes in the feature space and it can demonstrate the separation ability from the original feature data directly. The FLD is determined by optimizing the Fisher criterion $\tau(\omega) = \tau = \frac{\omega^T S_B \omega}{\omega^T S_W \omega}$, where S_B and S_W are the between-class and within-class scatter matrices [16]. The second step of the test is segmentation. As mentioned earlier, the K-means clustering method is applied to the weighted fused features to generate the final segmentation given the number of classes. Seeds for the K-means procedure are selected by using the first N feature vectors in raster order, where N represents the actual number of classes.

Table 2: *The value of τ by the five feature sets F_{G18}, F_{G24}, F_{C24}, F_{G18}^{C24} and F_{G24}^{C24} (see Table 1) for Fig. 2(a).*

τ by F_{G18}

	D002	D052	D068	D076	D034	D006
$D021$	1322.1	1467.3	738.9	1499.8	1211.3	1620.1
$D002$	-	983.5	161.5	503.8	780.2	1110.8
$D052$	-	-	1491.5	1485.9	2871.9	1567.8
$D068$	-	-	-	81.2	642.0	542.0
$D076$	-	-	-	-	406.6	504.8
$D034$	-	-	-	-	-	1365.3

τ by F_{G24}

	D002	D052	D068	D076	D034	D006
$D021$	1505.7	1565.8	792.1	1641.9	1794.0	1701.5
$D002$	-	1096.6	197.0	535.0	867.8	1207.6
$D052$	-	-	1513.9	1531.7	3153.3	1685.1
$D068$	-	-	-	88.6	666.8	565.1
$D076$	-	-	-	-	458.2	544.1
$D034$	-	-	-	-	-	1487.6

τ by F_{C24}

	D002	D052	D068	D076	D034	D006
$D021$	74.8	77.9	139.7	113.4	137.2	94.9
$D002$	-	3.4	40.6	17.5	52.9	19.8
$D052$	-	-	28.1	8.8	52.9	19.1
$D068$	-	-	-	8.2	191.6	21.5
$D076$	-	-	-	-	73.7	15.5
$D034$	-	-	-	-	-	60.5

τ by F_{G18}^{C24}

	D002	D052	D068	D076	D034	D006
$D021$	1949.7	1816.0	1006.7	1999.1	2177.0	1949.4
$D002$	-	1168.3	328.9	605.8	994.4	1631.2
$D052$	-	-	1994.1	1794.6	3298.3	1790.4
$D068$	-	-	-	112.8	1151.4	670.2
$D076$	-	-	-	-	538.1	576.1
$D034$	-	-	-	-	-	1946.5

τ by F_{G24}^{C24}

	D002	D052	D068	D076	D034	D006
$D021$	2199.8	1930.4	1084.4	2056.8	2636.3	2073.2
$D002$	-	1298.8	356.0	635.2	1084.9	1753.3
$D052$	-	-	2022.2	1844.9	3474.4	1918.4
$D068$	-	-	-	118.8	1172.7	687.8
$D076$	-	-	-	-	587.4	625.9
$D034$	-	-	-	-	-	2043.4

5.2 Discriminant Analysis

The FLD method is conducted to analyze the separability between the five feature sets (F_{G18}, F_{G24}, F_{C24}, F_{G18}^{C24} and F_{G24}^{C24}). A 32×32-pixel region is extracted from the center of each texture feature space to avoid influence of the boundary regions. Table 2 lists five sets of the FLD criterion τ for every possible pair of classes in Fig. 2(a). The fused feature sets (F_{G18}^{C24} and F_{G24}^{C24}) have significantly higher separation ability (an average more than 35%) than the three pure feature sets (F_{G18}, F_{G24} and F_{C24}). The co-occurrence features generate a noticeably lower separability compared to the other feature sets.

5.3 Segmentation

A demonstration of the image texture segmentation using the various feature sets outlined in Table 1 is presented in Fig. 2. The segmented results using the

pure feature sets (F_{G18}, F_{G24} and F_{C24}) are shown in Fig. 2 (b), (c) and (d) respectively. It can be seen from Fig. 2(b) that the *field stone* is segmented into two classes and *wood grain* is identified as the same class as *wire*. Fig. 2(c) shows an improvement by uniquely identifying the *field stone*, however, the *netting* is now split into two classes. Also, *woodgrain* and *wire* are still identified as a single class.

The worst result is produced using only the co-occurrence feature set (Fig. 2(d)), probably because this method captures only high frequency feature information. Here, only the *canvas* texture is identified properly. One could try to improve segmentation using additional co-occurrence features, however, there are two problems in achieving this. First, there is no known *a priori* method for selecting appropriate parameters to address all potential local frequencies and orientations. Second, using co-occurrence probabilities, larger windows can be used to capture lower frequency information, however, these same window sizes will capture all frequencies at the same time (not just the lower frequencies). In the Gabor case, the larger spatial bandwidth (ie. a larger window) is automatically associated with lower frequencies (by using the wavelet implementation) and such lower frequency filters only capture the center frequency of interest (ie. do not capture any other frequency information, unlike the co-occurrence method).

Fig. 2(e) shows the segmentation result by the fused feature set F_{G18}^{C24}. It is the most accurate result among all five results. Classes are properly recognized, however, there is some minor confusion in the boundary regions. Fig. 2(f) displays the result of the fused feature set F_{G24}^{C24}. The results are similar those obtained using F_{C24} (Fig. 2(c)).

Other texture images have been tested but the results are not presented here in consideration of the limited length of this paper. These results generally demonstrate that the fused feature set F_{G18}^{C24} can achieve more accurate segmentation results than the result by the three pure feature sets (F_{G18}, F_{G24} and F_{C24}) and the other fused feature set (F_{G24}^{C24}). That F_{G18}^{C24} generates improved segmentation compared to F_{G24}^{C24} was not fully expected based on the FLD results in Table 2. Here, F_{G24}^{C24} was demonstrated to have marginally improved separability compared to F_{G18}^{C24}. Perhaps the use of K-means (which does not account for class covariances) generates different class distinctions compared to FLD (which does utilize class covariance information). Further work into the use of clustering techniques that account for class covariances will be conducted to further improve the texture segmentation results.

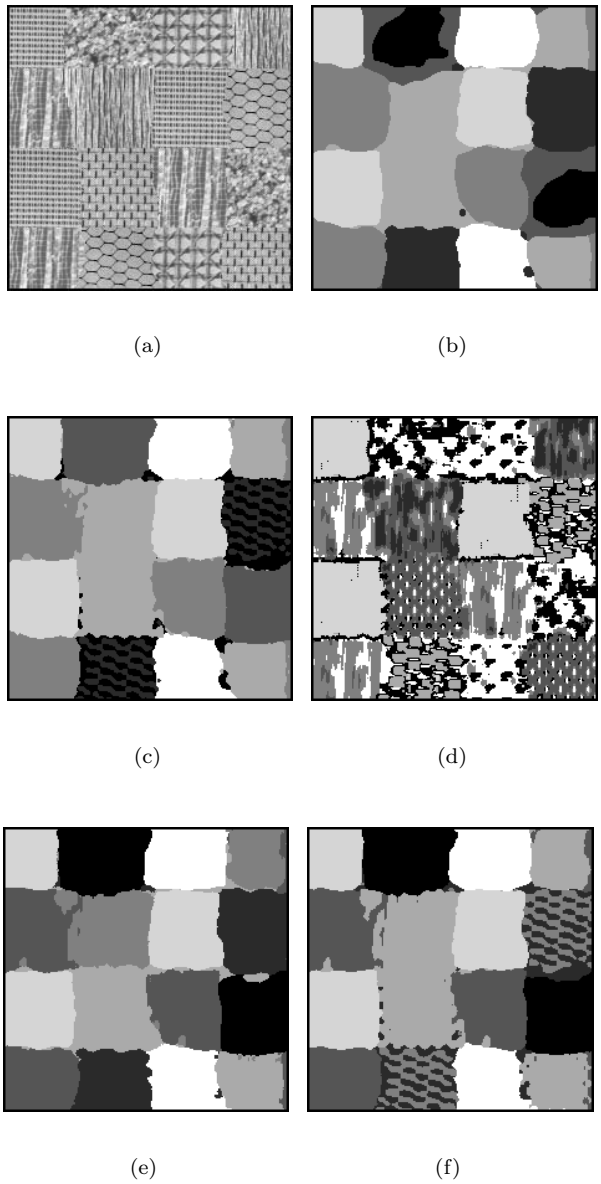

Figure 2: *(a) The original image. The other figures (b)-(f) display segmentation results based on the configurations identified in Table 1. (b) Result for F_{G18}. (c) Result for F_{G24}. (d) Result for F_{C24}. (e) Result for F_{G18}^{C24}. (f) Result for F_{G24}^{C24}. The best result is (e).*

6 Conclusion and Discussion

This paper presents a design-based method to fuse Gabor filter texture features and co-occurrence probability features. The fusion is based on the theoretical analysis of each method so as to combine robust and reliable features. Discriminant analysis of

the fused features indicates significant improvement over the individual methods. The fused features are then weighted by the feature contrast method for the K-means clustering segmentation. Experiments demonstrate more accurate segmentation results by the weighted fused features than the other features.

Acknowledgements

The authors thank GEOIDE (Geomatics for Informed Decision) and CRYSYS (Cryosphere System in Canada) for financial support of this project.

References

[1] M. Tuceryan and A. K. Jain, *Handbook of Pattern Recognition and Computer Vision, Chapter 2: Texture Analysis*, World Scientific, Singapore, 1993.

[2] D. Weszka, C. R. Dyer, and A. Rosenfeld, "A Comparative Study of Texture Measures for Terrain Classification," *IEEE Trans. Systems, Man and Cybernetics*, vol. 6, no. 4, pp. 269–285, 1976.

[3] R. W. Conners and C. A. Harlow, "A Theoretical Comparison of Texture Algorithms," *IEEE Trans. Pattern Anal. Machine Intell.*, vol. 2, no. 5, pp. 204–221, 1980.

[4] A. K. Jain and F. Farrokhnia, "Unsupervised Texture Segmentation Using Gabor Filters," *Pattern Recognition*, vol. 24, no. 12, pp. 1167–1186, 1991.

[5] A. H. S. Solberg and A. K. Jain, "Texture Fusion and Feature Selection Applied to SAR Imagery," *IEEE Trans. Geoscience and Remote Sensing*, vol. 35, no. 2, pp. 475–479, 1997.

[6] D. A. Clausi, "Comparison and Fusion of Co-occurrence, Gabor and MRF Texture Features for Classification of SAR Sea-Ice Imagery," *Atmosphere-Ocean*, vol. 39, no. 3, pp. 183–194, 2000.

[7] D. H. Hubel and T. N. Wiesel, "Receptive Fields and Functional Architecture in Two Nonstriate Visual Areas 18 and 19 of the Cat," *J. Neurophysiol*, vol. 28, pp. 229–289, 1965.

[8] F. W. Campbell and J. G. Robson, "Application of Fourier Analysis to the Visibility of Gratings," *J. Physiol.*, vol. 197, pp. 551–566, 1968.

[9] A. R. Rao and G. L. Lohse, "Identifying High Level Features of Texture Perception," *CVGIP: Graphical Models and Image Processing*, vol. 55, no. 3, pp. 5218–5233, 1993.

[10] A. C. Bovik, M. Clark, and W. S. Geisler, "Multichannel Texture Analysis Using Localized Spatial Filters," *IEEE Trans. Pattern Anal. Machine Intell.*, vol. 12, no. 1, pp. 55–73, 1990.

[11] D. A. Clausi and M. E. Jernigan, "Designing Gabor Filters for Optimal Texture Separability," *Pattern Recognition*, vol. 33, no. 0, pp. 1835–1849, 2000.

[12] R. M. Haralick, K. Shanmugam, and I. Dinstein, "Textural Features for Image Classification," *IEEE Trans. Sys. Man Cybern*, vol. 3, pp. 610–621, 1973.

[13] D. G. Barber and E. F. LeDrew, "SAR Sea Ice Discrimination Using Texture Statistics: A Multivariate Approach," *Photogrammetric Engineering and Remote Sensing*, vol. 57, no. 4, pp. 385–395, 1991.

[14] L. K. Soh and C. Tsatsoulis, "Texture Analysis of SAR Sea Ice Imagery Using Gray Level Co-occurrence Matrices," *IEEE Trans. Geoscience and Remote Sensing*, vol. 37, no. 2, pp. 780–795, 1999.

[15] D. A. Clausi, "An Analysis of Co-occurrence Texture Statistics as A Function of Grey Level Quantization," *Canadian J. Remote Sensing*, vol. 28, no. 1, pp. 1–18, 2002.

[16] R. O. Duda and P. E. Hart, *Pattern Classification and Scene Analysis*, A Wiley-Interscience Publication, USA, 1973.

[17] O. Pichler, A. Teuner, and B. J. Hosticka, "An Unsupervised Texture Segmentation Algorithm with Feature Space Reduction and Knowledge Feedback," *IEEE Trans. Image Processing*, vol. 7, no. 1, pp. 53–61, 1998.

[18] P. Brodatz, *Texture–A Photographic Album for Artists and Designers*, Reinhold, New York, USA, 1968.

[19] J. Bigun and J. M. du Buf, "N-folded Symmetries by Complex Moments in Gabor Space and Their Applications to Unsupervised Texture Segmentation," *IEEE Trans. Pattern Anal. Machine Intell.*, vol. 16, no. 1, pp. 80–87, 1994.